Driving Forces of Protein Association: The Dimer-Octamer Equilibrium in Arylsulfatase A

Peter Vagedes, Wolfram Saenger, and Ernst-Walter Knapp
Institut für Chemie, Fachbereich Biologie, Pharmazie, Chemie, Freie Universität Berlin, D-14195 Berlin, Germany

ABSTRACT The enzyme arylsulfatase A (ASA) occurs in solution as dimer (α_2) above pH 6 and associates to octamers $(\alpha_2)_4$ below pH 6. The crystal structure of ASA suggests that the (α_2)-$(\alpha_2)_4$ equilibrium is regulated by protonation/deprotonation of Glu-424 located at the interface between (α_2) dimers in the octamer. The reason for this assumption is that Glu-424 can be in two different conformers where it forms an intra or intermolecular hydrogen bond, respectively. In the present study we investigate this protein association process theoretically. The electrostatic energies are evaluated by solving the Poisson-Boltzmann equation for the inhomogeneous dielectric of the protein-water system for the dimer and octamer configurations. If a conventional surface energy term is used for the nonelectrostatic interactions, the absolute value of free energy of association fails to agree with experiment. A more detailed treatment that explicitly accounts for hydrophilic and hydrophobic character of the amino acids in the dimer-dimer interface of the octamer can explain this discrepancy qualitatively. The pH dependence of the computed association energy clearly demonstrates that the octamer is more stable at low pH if Glu-424 becomes protonated and forms an intermolecular hydrogen bond. We found a slight preference of Glu-424 to be in a conformation where its acidic group is fully solvent-exposed in the dimer state to form hydrogen bonds with water molecules. Application of the proton linkage model to calculate the association energy from the simulated data yielded results identical to the one obtained from the corresponding direct method.

INTRODUCTION

Protein-protein association plays an important role in living cells because it is involved in all kinds of regulation, recognition, signal transduction, and intermolecular transport processes (Gavin et al., 2002). It requires that proteins bind to each other in a specific manner. To understand these processes we must know the forces that drive protein-protein association and regulate it by external parameters. In particular, electrostatic forces have an influence on strength and specificity of binding and on the rates of association.

Human arylsulfatase A (ASA, EC 3.1.6.8) is an enzyme that occurs in the lysosome of the human cell, where acidic pH values prevail. ASA forms homo-octamers in an acidic environment (pH $\leq$ 6) and dissociates to homo-dimers at higher pH values. This pH-regulated protein association/dissociation suggests that it may be governed by the protonation/deprotonation equilibrium of titratable groups and renders ASA a very attractive model system to study the mechanism of protein-protein association processes in more detail.

In the present work we describe how the pH-dependent association free energies between dimers of ASA can be understood on the basis of electrostatic interactions. We outline what is known biochemically about ASA and its association process and give the theoretical framework and technical details necessary to compute the energetics of the association process. Finally, we present and discuss the mechanism of the dimer-octamer association of ASA.

Function of arylsulfatase A

ASA is a hydrolytic enzyme. Its major physiological substrate is cerebroside 3-sulfate, a sphingolipid sulfate ester that is part of the myelin sheet (Fig. 1). The name arylsulfatase refers to the capability of ASA to also hydrolyze synthetic arylsulfates with even higher rates than natural substrates.

ASA belongs to the sulfatase family. The members of this family hydrolyze sulfate ester bonds of a variety of compounds, including mucopolysaccharides, cerebrosides, and steroids. Among sulfatases, ASA has been studied most extensively. With the other eight known human sulfatases it shares a high sequence similarity of 47–59% (Franco et al., 1995). Seven human disorders are associated with a deficiency in one of the sulfatases (Neufeld and Muenzer, 1995). Deficiency of ASA leads to metachromic leukodystrophy (MLD), a disease where sulfate esters of galactocerebrosides accumulate in several organs (Ballabio and Shapiro, 1995; Kolodny and Fluharty, 1995).

The key residue for the activity of sulfatases is an unusual C_α-formylglycine that results from a posttranslational oxidation of a cysteine (Cys-69 in ASA; Dierks et al., 1997). The newly synthesized enzyme is inactive if the posttranslational modification of this cysteine does not occur.

In an acidic environment at ~pH 5, ASA shows optimal catalytic activity and human ASA occurs as homo-octamer, whereas at neutral and alkaline pH it exists as a homodimer. A similar dissociation/association behavior is reported for ox liver arylsulfatase (Jerfy et al., 1976; Nichol

Submitted May 1, 2002, and accepted for publication June 13, 2002.

Address reprint requests to Ernst-Walter Knapp, Freie Universität Berlin, Takustrasse 6, D-14195 Berlin, Germany. Tel.: 49-30-8384387; Fax: 49-30-8385346; E-mail: knapp@chemie.fu-berlin.de.

0006-3495/02/12/3066/13 $2.00

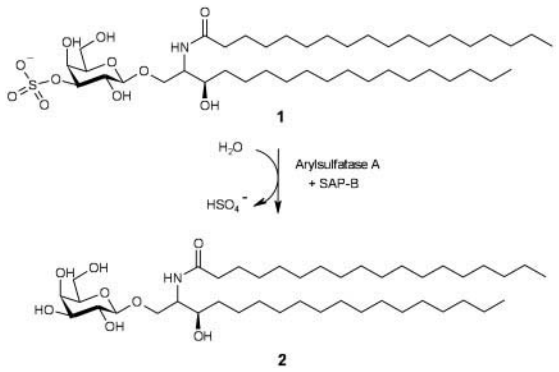

FIGURE 1 Hydrolysis of the natural substrate of ASA, cerebroside 3-sulfate (1), to galactosyl ceramid (2). A sphingolipid activator protein (SAP-B) is needed as a cofactor to enlarge the solubility of the sphingolipid.

and Roy, 1965; Nichol and Roy, 1966) and rabbit liver arylsulfatase (Waheed and van Etten, 1979). It has been shown that the association between ASA monomers to form dimers and then octamers is also found in arylsulfatases isolated from different species (Waheed and van Etten, 1985), suggesting that the interface structure between these enzymes may be conserved.

Structure of ASA

In 1998 the crystal structure of ASA was published (Lukatela et al., 1998). The globular ASA monomer consists of 489 residues and is hat-shaped with a base of $70 \cdot 45$ Å^2 and a height of 50 Å (Fig. 2). The secondary structure of ASA is of the mixed α/β-type. The enzyme contains a Mg^{2+} ion in the active site which, together with the formylglycine residue 69, is located in the catalytic cavity. The ASA

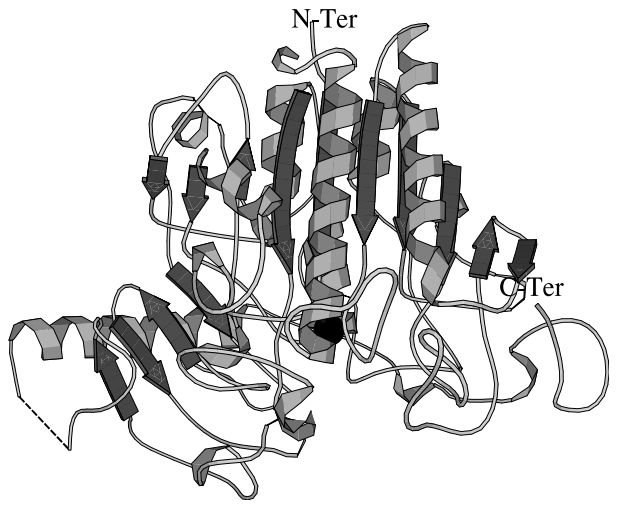

FIGURE 2 Structure of the ASA monomer. The magnesium ion in the active site is depicted as black sphere in the lower part of the structure. The picture was drawn with Molscript (Kraulis, 1991).

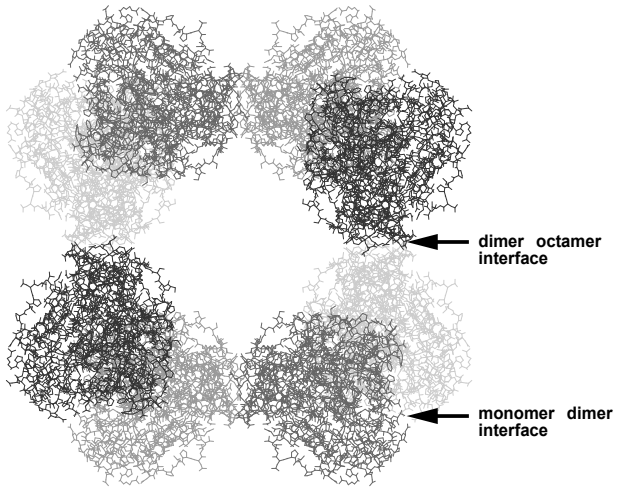

FIGURE 3 ASA octamer in the crystal structure composed of four homodimers. Each homodimer consists of one monomer in light gray in the back and one in dark gray in front. The picture was drawn with Molscript (Kraulis, 1991).

monomer has significant structural analogy to alkaline phosphatase (AP) (Coleman, 1992; Vallee and Auld, 1993), which is also a hydrolytic enzyme containing two zinc ions in the active site, but no formylglycine.

The x-ray structure (Lukatela et al., 1998) was determined from crystals that were grown at acidic pH (5.0–5.4). They consist of ASA homo-octamers $(\alpha_2)_4$ (Fig. 3) that are composed of four homo-dimers (α_2). The monomers (α) in the octamer are related by the symmetry elements of point group 422 (D_4).

In the octamer there are two different monomer-monomer contact surfaces I and II. The larger contact surface area [interface (I)] of 1600 Å^2 connects the monomers in the homo-dimers (Fig. 4). Within this contact surface there are 2×3 direct hydrogen bonds between the monomers and 2×25 hydrogen bonds mediated by water molecules. Despite this small number of direct interactions the resulting interaction energy is so strong that the dimer was previously even described as a monomer (Nicholls and Roy, 1971). A large part of stabilization of the dimer results from hydrophobic interactions.

The smaller contact surface [interface (II)] that covers 900 Å^2 allows for the dimer-dimer cohesion and is formed mainly by hydrophobic interactions between the aliphatic amino acids of two nearly antiparallel α-helices (Fig. 5) assisted by 2×3 direct hydrogen bonds between the dimers and additional hydrogen bonds mediated by 2×9 trapped water molecules.

PROTEIN-PROTEIN ASSOCIATION

General aspects

The association of proteins was often compared to the folding process of proteins. Protein-protein association is a

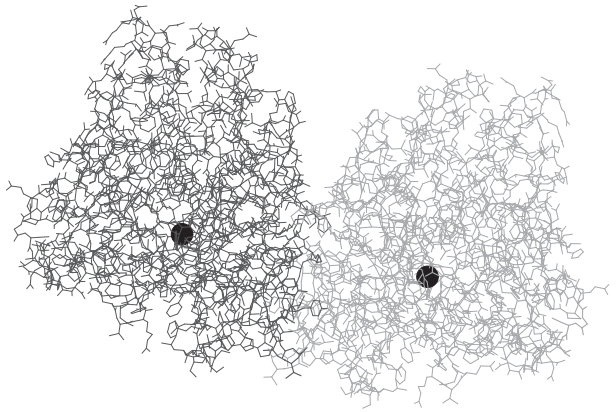

FIGURE 4 The ASA homodimer. The contact surface (I) between adjacent monomers is 1600 Å^2. The magnesium ions located in the active site are depicted as black spheres. There are 2 × 3 direct hydrogen bonds between the two monomers: His-328–N_ϵ----O–Pro-42 (3.4 Å), Ser-43–O_γ----O–Ser-432 (2.6 Å), and Tyr-439–O_η----O_γ–Thr-408 (2.9 Å). In addition, 2 × 25 water molecules in the contact region mediate hydrogen bonds. The picture was drawn with Molscript (Kraulis, 1991).

very specific process. It occurs via well-defined protein interfaces that evolved to accomplish the recognition and binding process (Gavin et al., 2002). The composition of amino acids at protein-protein interfaces differs from the one within protein cores (Jones and Thornton, 1996; Larsen et al., 1998; Lo Conte et al., 1999). In the protein core hydrophobic residues dominate. They are most relevant for protein folding and stability. At protein surfaces polar and charged residues prevail to guarantee solubility.

The role of amino acids at protein-protein interfaces is twofold. They should promote protein-protein association, but they should also allow proteins to be soluble, if they are not associated. Hydrophobic residues at the protein surface favor association. However, they do this unspecifically, allowing many different configurations. Hydrophilic residues disfavor association, but they can act specifically such that charged residues form intermolecular salt bridges and polar residues form intermolecular hydrogen bonds. These interactions allow for interfacial recognition of protein surfaces and lead to a definite configuration of the associated proteins. This is why the concentration of hydrophilic residues on protein surfaces involved in association may be less than for solvent-exposed surfaces, but may be larger than in the protein interior. Hence, protein-protein association is driven by a significant contribution from hydrophobic forces at the interface, albeit these forces are generally smaller than in protein folding.

A fundamental difference between protein folding and protein-protein association is the amount of entropy loss that accompanies them. The conformational entropy penalty associated with protein folding is much larger than the one for protein-protein association, where only translational and rotational entropy of relative motion vanishes. The entropy loss of side chains at protein-protein interfaces is small compared to the number of residues that lose conformational entropy during protein folding. In summary, the forces that control the association of proteins are generally not as large as the forces that are responsible for protein folding. In cases where they are larger, they would interfere with protein folding at higher concentrations and lead to partial unfolding associated with unspecific aggregation.

It is known that the formation of salt bridges and hydrogen bonds in the interior of a protein is generally less favorable and even disfavors the folding of a protein (Gilson et al., 1985; Hendsch and Tidor, 1994; Honig and Hubbell, 1984; Honig and Nicholls, 1995; Yang and Honig, 1995). The reason for this phenomenon is the desolvation energy: the formation of an ion pair within the protein interior requires the removal of the charged or polar moieties from water, including the destruction of their solvent shells. The desolvation costs associated with this process cannot be compensated by the pairwise Coulomb interaction (Parseghian, 1969).

Initially, it was assumed that electrostatic interactions also oppose protein-protein association processes for the

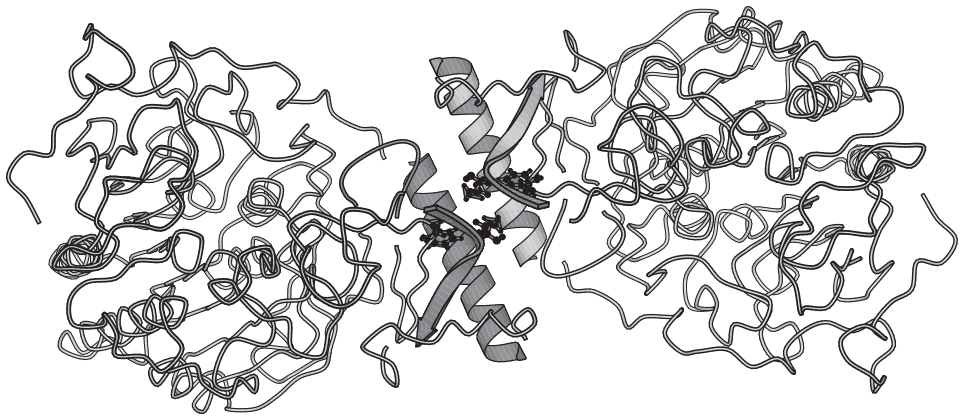

FIGURE 5 Contact region between two "secondary" dimers (II) of ASA. Only the relevant monomers are depicted. Two antiparallel α-helices are the major constituents of the adhering surfaces. The "secondary" dimer contact surface (II) covers an area of 900 Å^2. There are 3 × 2 direct hydrogen bonds between the two dimers: Lys-457–N_ζ----O–Glu-382 (3.0 Å), Lys-457–N_ζ----O–Asp-467 (3.0 Å), and Glu-424–O_ϵ----O–Phe-398 (2.9 Å). In addition there are 2 × 9 water molecules in the contact region that mediate hydrogen bonds. The picture was drawn with Molscript (Kraulis, 1991).

same reasons, but growing evidence suggests that polar groups can contribute in some cases favorably to the stabilization of protein complexes (Sheinerman et al., 2000). Theoretical investigations showed that electrostatic interactions can have a stabilizing effect on protein-protein binding (Xu et al., 1997) but also a destabilizing effect (Reddy et al., 1998; Schapira et al., 1999). There, it was argued that the polar environment in protein-protein interfaces allows a more favorable electrostatic interaction than is possible in hydrophobic protein cores. This is comparable to the situation in hyperthermophilic proteins, where networks of electrostatic interactions account for enhanced thermal stability (Xiao and Honig, 1999).

In fact, mutagenesis experiments showed that replacing individual polar and charged groups by alanine destabilizes protein-protein complexes (Bogan and Thorn, 1998). However, these experiments do not show whether the interplay of polar and charged interactions stabilizes or destabilizes protein-protein complexes. If one partner of an ion pair is removed and the complex is destabilized, this demonstrates that the corresponding residue is stabilizing the complex when the other charged group is present. However, the actual comparison has to be made with the reference state consisting of two isolated charged or polar monomers. In the discussion of protein folding it has been shown that the removal of only one member of an isolated hydrogen-bonded pair or ion pair destabilizes the native protein structure, even if the hydrogen bond or the ion pair itself is destabilizing (Honig and Yang, 1995).

Hence, it is still unclear to which extent electrostatic interactions can contribute to the stabilization of protein-protein complexes. However, it is known that electrostatic fields around proteins can enhance the rates of protein-protein association (Elcock et al., 1999; Getzoff et al., 1992; Sharp et al., 1987) and that electrostatic interactions have an influence on the specificity of protein-protein binding.

Association of arylsulfatase

The dimer-octamer equilibrium of ASA is regulated by the pH. ASA dimers associate to octamers when the pH is below 6. It has been proposed earlier that this regulation is exerted by the protonation/deprotonation equilibrium of a titratable carboxylate or histidine side chain (Nichol and Roy, 1966; Nicholls and Roy, 1971). The only acidic side chain at the dimer-dimer interface (II) is Glu-424, which might act as a switch. The two Glu-424 in the dimer-dimer interface (II) are only 5 Å apart if they are in the conformation to form intramolecular hydrogen bonds and are found twofold disordered in the electron density map (see Figs. 6 and 7).

The dimer-octamer equilibrium may be explained by a switch function of Glu-424. Below pH 6, Glu-424 becomes protonated and stabilizes the octamer due to an intermolecular hydrogen bond to Phe-398–O from the adjacent dimer.

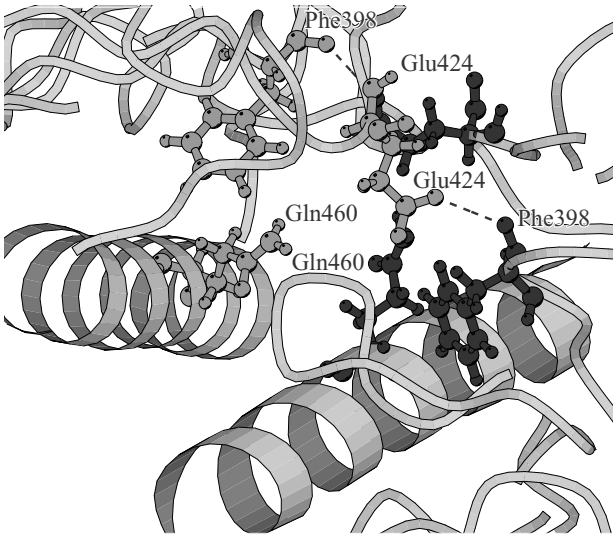

FIGURE 6 Hydrogen bonds at the dimer-dimer interface. The conformation is shown in which the Glu-424 side chain and the backbone carbonyl group of Phe-398 from different monomers form hydrogen bonds with each other. All residues at the dimer-dimer interface (II) involved in intra and intermolecular hydrogen bonds are shown. Residues from different subunits are displayed in dark gray and light gray, respectively. The picture was drawn with Molscript (Kraulis, 1991).

At pH 7, Glu-424 is deprotonated and the hydrogen bond to Phe-398–O is no longer possible. Moreover, the octamer will be destabilized by the electrostatic repulsion between the two charged Glu-424 that are only 5 Å apart. In the deprotonated form, the preferred conformation of Glu-424 is the one that allows for an intramolecular hydrogen bond

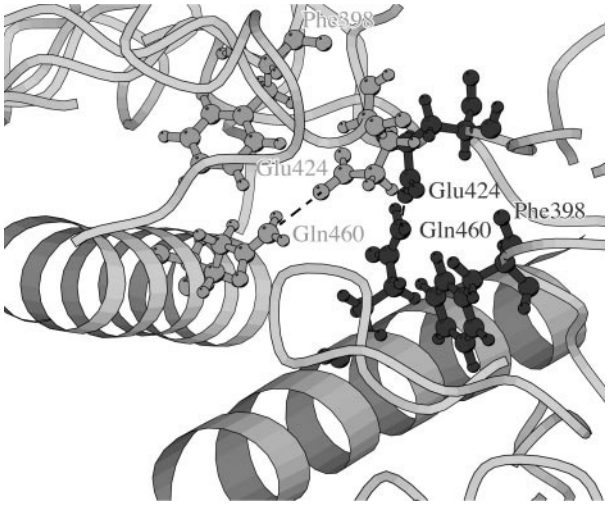

FIGURE 7 Hydrogen bonds at the dimer-dimer interface. The conformation is shown in which the side chain of Glu-424 and the NH_2 group of Gln-460 from the same monomers form hydrogen bonds with each other. This conformation can be generated from the one displayed in Fig. 6 by rotating the Glu-424 side chain around the C_β–C_γ bond. For more details see the caption to Fig. 6.

to Gln-460. With this argument the electrostatic interactions and the protonation/deprotonation equilibria are the most important factors for the regulation of the association process of ASA. To investigate the association behavior within the light of this hypothesis it is necessary to account for the protonation probability of Glu-424 in the dimer and in the octamer configurations, and the free energy of association at various pH values.

In this work we modeled the association of ASA dimers to octamers by considering the association of two monomers that form the dimer-dimer interface (II) as mentioned above. To investigate the role of Glu-424 upon association of the protein monomers, both possible conformations of this residue, as they are shown in Figs. 6 and 7, were considered. 1) Glu-424 in the conformation suitable for the intramolecular hydrogen bonds to Gln-460; 2) Glu-424 in the conformation suitable for the intermolecular hydrogen bonds to Phe-398.

THEORETICAL FRAMEWORK

Computation of energies

The protonation pattern of a protein with N_t titratable groups can be characterized by a protonation state vector

$$\vec{n} = (x_1, x_2, \ldots x_{N_t}). \quad (1)$$

The component x_μ of $\vec{n}$ adopts the values 1 or 0 depending on whether titratable group μ is protonated or not. The energy of a protein in conformation ℓ with N_t titratable groups ν, μ in protonation state $\vec{n}$ is evaluated as

$$G^{n,l} = \sum_{\mu=1}^{N_t} (x_\mu^{n,l} - x_\mu^{0,l}) k_B T \ln 10(\mathrm{pH} - \mathrm{pK}_{a,\mu}^{intr,l}) + \sum_{\nu>\mu=1}^{N_t} (x_\mu^{n,l} + z_\mu^0)(x_\nu^{n,l} + z_\mu^0) W_{\mu\nu}^l + \Delta G_{conf}^l \quad (2)$$

where $\mathrm{pK}_{a,\mu}^{intr,1}$ is the intrinsic pK_a value of titratable group μ in the protein with all other titratable groups in the reference protonation state ($\vec{n} \equiv \vec{0}$, with $x_\mu^{o,1}$), where all titratable groups are in the neutral charge state that is protonated for acidic ($z_\mu^0 = -1$) and deprotonated for basic ($z_\mu^0 = 0$) residues. The parameter z_μ^0 accounts for the formal unit charge of titratable residue μ in the deprotonated state. Only histidine was chosen to be protonated in the reference state to overcome the ambiguity problem of neutral His, where a proton is bound to N_δ or N_ϵ. Note that with the above definition of the electrostatic energy the zero point on the energy scale is at the reference protonation state. $\Delta G_{conf}^l = \Delta G_{conf}^l - \Delta G_{conf}^r$ is the energy difference between a fixed but arbitrary reference conformation r and the actual conformation l, where both energies are evaluated in the reference protonation state.

The electrostatic approach presented above can only account for electrostatic energy changes that are due to differences in the environment (protein or aqueous solution) of a considered titratable molecular group and result in a corresponding calculated shift of the pK_a value. To obtain absolute pK_a values, the electrostatic energy of the titratable molecular group (the so-called model compound) must also be evaluated for a dielectric medium corresponding to aqueous solution and be matched with the experimental known pK_a value. For a titratable amino acid the model compound exists in the corresponding monomeric amino acid, which is neutralized by methylating the amide group and amidating the acidic group. For more details see Ullmann and Knapp (1999).

Equation 2 requires the calculation of the relative conformational energy ΔG_{conf}^l in addition to the terms required for the calculation of the protonation pattern of a single conformation. This relative conformational energy consists of three parts

$$\Delta G_{conf}^l = \Delta G_s^l + \Delta G_{FF}^l + \Delta G_{NE}^l. \quad (3)$$

In Eq. 3, ΔG_S^l denotes the electrostatic contribution to the solvation energy difference of conformation l relative to the reference conformation r. The energy term ΔG_{NE}^l accounts for the nonelectrostatic contribution to the solvation energy difference. In ΔG_{FF}^l, the Coulomb energy differences between conformations l and r corresponding to a classical molecular mechanics force field are summarized. The calculation of the electrostatic contribution to the solvation energy of the various conformations can be done from numerical results of the linearized Poisson-Boltzmann equation (LPBE). It is the energy required to transfer the protein in each conformation (ℓ) from a homogeneous dielectric (hom) medium with $\epsilon_S = \epsilon_P$ and vanishing ionic strength to the corresponding inhomogeneous (inhom) dielectric with nonvanishing ionic strength. The corresponding energy expression is given by

$$G_S^l = \frac{1}{2} \sum_{i=1}^{N_P} q_{i,P}(\phi_P^{inhom}(\mathbf{r}_i^l, q_P) - \phi_P^{hom}(\mathbf{r}_i^l, q_P)) \quad (4)$$

The solvation energy represents the interaction of the N_p protein charges with their own induced reaction field in the corresponding dielectric medium. The term $\phi_P^{inhom}(\mathbf{r}_i^l, q_P)$ denotes the electrostatic potential at position $\mathbf{r}_i^l$ for the inhomogeneous dielectric, whereas $\phi_P^{hom}(\mathbf{r}_i^l, q_P)$ is the electrostatic potential in the homogeneous dielectric. In the homogeneous and inhomogeneous dielectric system the electrostatic potentials are calculated from all atomic charges $q_{i,P}$ in the protein, where all titratable groups are in the reference protonation state. G_S^r is calculated analogously. The nonelectrostatic contribution ΔG_{NE}^l in Eq. 3 to the solvation energy of both conformations is assumed to be proportional to the solvent-accessible surface area (Chothia,

1976; Eisenberg and McLachlan, 1986; Nozaki and Tanford, 1971; Zhang and Koshland, 1996)

$$\Delta G^{l}_{NE} = \gamma(A^{l} - A^{r}), \quad (5)$$

where A^{l} and A^{r} are the solvent-accessible surfaces of the reference conformation r and the actual conformation l, respectively. The surface energy parameter γ is determined empirically (Sitkoff et al., 1994).

Monte Carlo sampling of conformations

The protonation probability of a titratable group depends on the pH. The conformation of side chains of titratable groups may depend on the pH and may thus have an influence on the protonation state of the titratable groups. This becomes obvious by inspecting Eq. 2, where the energy difference between the considered conformation and the reference conformation of the molecular system contributes to the total energy. In the present application, we will use the notion *conformation* also collectively for the monomer and "secondary" dimer configuration as well as for the conformations of Glu- 424. Although this is chemically incorrect, it allows us to describe the usage of the theoretical machinery to simulate the dimer-octamer association of ASA more easily.

The protonation pattern of two protein monomers can be established for the isolated monomers and for the monomers associated to the corresponding dimer. With the Monte Carlo (MC) Metropolis importance sampling of states one obtains the population probability of each association state. The free energy difference between the isolated monomers and the dimer is then given by

$$\Delta G_{ass} = -k_B T \ln \frac{\langle \text{monomer} \rangle}{\langle \text{dimer} \rangle}, \quad (6)$$

where ΔG_{ass} is the association free energy and $\langle$monomer$\rangle$ and $\langle$dimer$\rangle$ are the population probabilities of the monomer and the dimer configuration, respectively.

The proton linkage model

The electrostatic energy of association is calculated by two methods in this study. First, the populations of the two configurations are investigated by an MC importance sampling of conformations, yielding the population distribution between monomers and dimers. With proper inclusion of the correct reference energies this yields, in principle, the absolute free energy of association. As an alternative approach the application of the proton linkage model is presented here. Within this method the free energy of association is determined in dependence on the pH value. Although, with appropriate experimental information in this approach, absolute values of association energies can be calculated for different pH values.

The association constant of a protein binding process can be measured via the proton release/uptake of the system accompanying the binding. This has been done frequently in experimental investigations (Lebovitz and Laskowsky, 1962; Mauk et al., 1991, 1994; van Vlijmen et al., 1998; Wyman, 1964) The proton release/uptake can also reveal the free energy changes going along with processes like redox reactions (Beroza et al., 1995; McPherson et al., 1988) and protein unfolding (Beroza et al., 1995; McPherson et al., 1988; Schaefer and Karplus, 1997; Tanford, 1970; Yang, 1993).

The proton release/uptake associated with a process can be used to determine free energies by applying the so-called *proton linkage model*. This model relates the pH-dependence of an equilibrium constant to proton release/uptake. Hence, the proton linkage model can be used to investigate the pH-dependence of processes like redox-reactions, conformational transitions, and binding of proteins.

The theory underlying the proton linkage model can be developed as follows. The association process between two proteins is described by the reaction equation

$$A + B \Leftrightarrow AB; \quad K_A = \frac{[AB]}{[A][B]}, \quad (7)$$

where K_A represents the equilibrium constant of association. The proteins A and B and the protein-protein complex AB can exist in L_A, L_B, and L_{AB} different protonation states, respectively. The total concentration of each species is then given as the sum over all protonation states and Eq. 7 reads

$$K_\Lambda = \frac{\sum_{i=0}^{L_{AB}} [(AB)_i]}{\sum_{i=0}^{L_A} [A_i] \sum_{i=0}^{L_B} [B_i]}, \quad (8)$$

where $[A_i]$, $[B_i]$, and $[(AB)_i]$ denote the concentration of A, B, and AB in the respective protonation state i. As the concentrations $[A_i]$, $[B_i]$, and $[(AB)_i]$ vary with pH, K_A is also pH-dependent. It was shown that the equilibrium constant K_A depends on the total proton release/uptake between two pH values as (Laskowsky and Finkenstadt, 1972)

$$\lg K_A(pH_2) = \lg K_A(pH_1) + \int_{pH_1}^{pH_2} \Delta n(pH) d pH. \quad (9)$$

According to Eq. 9, the logarithm of the equilibrium constant of association $K_A(pH_2)$ at pH_2 can be obtained by adding the number of protons Δn(pH) that are released between pH_1 and pH_2 to the logarithm of the equilibrium constant at pH_1. The numerical integration can, for instance, be performed with Simpson's rule. From the equilibrium constant, the pH dependence of the free energy of association can be calculated as follows

$$\Delta G_{12} = G(pH_2) - G(pH_1),$$

$$\text{where} \quad G(pH) = -k_B T \ln[K_A(pH)]. \quad (10)$$

Note that in order to compute the number of protons released upon association the MC titration can be performed for the monomer and dimer state separately. Hence, no problems with the sampling of the monomer and dimer configurations can occur.

METHODS

Preparation of atomic coordinates

The crystal structure of ASA was determined at a resolution of 2.1 Å and is deposited as entry 1auk in the Protein Data Bank with atomic coordinates for one monomer. The 18 N-terminal amino acids belong to a signal peptide, which is not present in the mature protein and in the crystal structure. Hence, these residues were not considered in this study. Moreover, the residues Gly-444 to Gly-447 and Asp-504 to Ala-507 could not be identified from x-ray structure analysis due to poorly defined electron density. They were modeled into the structure with the program CHARMM (Brooks et al., 1983). Hydrogen atoms were added to the structure using the HBUILD facility of CHARMM. The structure was then energy-minimized with the CHARMM22 force field (MacKerrell et al., 1998) by a protocol that fixed all atoms whose positions are known from the crystal structure. Thus, only atoms that were added by modeling have coordinates generated by the applied force field and in agreement with the known structure.

The "secondary" dimer that results from the association of monomers via the dimer-dimer interface (II) was generated with the program PDBSET from the CCP4 (Collaborative Computational Project Number 4, 1994) program suite by applying the corresponding twofold symmetry operation. After the creation of the "secondary" dimer all hydrogen atom positions were energy-minimized again such that the hydrogen atoms adopted their position in agreement with the dimer structure.

Although the x-ray structure was determined at acidic pH values (pH 5.0–5.4), where ASA exists as octamer, the conformation of Glu-424 in the PDB entry is the one corresponding to the dimer, with Glu-424 forming an intramolecular hydrogen bond to Gln-460. The intermolecular hydrogen bond was modeled with the program CHARMM by rotating the side chain around the bonds C_β–C_γ and C_γ–C_δ such that the distance between the protonated carboxylate oxygen of Glu-424 and the backbone oxygen of Phe-398 became 3.1 Å. This was done in both monomers forming the "secondary" dimer. The distance of 3.1 Å is the shortest possible distance between the partners of the intermolecular hydrogen bond without applying additional restraints on the "secondary" dimer. The side chain of Glu-424 was then also energy-minimized while fixing the atoms of all residues but Glu-424.

The described modeling procedure yielded four different structures. The abbreviations in capital letters are used in the figures below (see Figs. 6 and 7). 1) Two different monomer conformations: one with Glu-424 in a conformation suitable for the intramolecular hydrogen bond (MONO/GLU-INTRA), the other with Glu-424 in a conformation to form the intermolecular hydrogen bond (MONO/GLU-INTER). 2) Two "secondary" dimer conformations, which consist of monomers with the same Glu-424 conformations DIMER/GLU-INTRA and DIMER/GLU-INTER.

In the crystal structure, 2×9 water molecules were found that form hydrogen bonds within the interface (II) of the "secondary" dimer. Although water molecules in the dimer interface (II) contribute to the association energy, they were not considered explicitly in the present study, and removed. In the cavities resulting from the removed water molecules the dielectric constant was set to $\epsilon_S = 80$. The surface charges generated at the interfaces between a medium of low and high dielectric constant mimic the electrostatic interactions that result from hydrogen bonds. For similar reasons, all solvent molecules were represented implicitly by the dielectric medium. For a more detailed discussion see Ullmann and Knapp (1999). This procedure avoids the problem that the positions of the bound water molecules may differ in the monomer and dimer state, which facilitates a proper definition of reference conformations.

Evaluation of electrostatic energies

For the electrostatic energy computations of the dimer-octamer association, the LPBE of the associated protein complexes need to be solved numerically several times. In this procedure, all values of the atomic charges, dielectric constant, and electrostatic potential of the protein complex are mapped onto a grid. Because a suitable grid for the octamer would be too large to solve the LPBE in a conventional work station, only the relevant part of the octamer was considered in this study. The association of ASA dimers to octamers occurs at the smaller 900 $Å^2$ interface (II) between (α_2) dimers. To save computer power, the dimer-dimer association was actually simulated with two monomers associating via the corresponding interface (II). This "secondary" (artificial) dimer has to be distinguished from the "primary" dimer, which is in equilibrium with octamers and predominates at higher pH values, as explained in the previous section. The "secondary" dimers do not exist isolated in solution but serve as a model system in the present computations. In this way, the system size can be considerably reduced such that the electrostatic energies can be solved with moderate requirements on computer memory and CPU time.

The electrostatic potentials that were required for the titration of the ASA structures were calculated by solving the LPBE with the program MULTIFLEX from the MEAD software package (Bashford, 1997; Bashford and Gerwert, 1992). The atomic partial charges of the different molecular groups including the titratable residues were taken from the CHARMM22 force field (MacKerrell et al., 1998). For some titratable amino acids (Arg, Cys, Tyr, C-ter, and N-ter) charges are available only for the standard protonation state. Here, we used quantum chemically computed charges, which are given in the supporting information of Rabenstein et al. (1998). For the heterogeneous dielectric of a protein-water system, the dielectric constant for the solvent was chosen to be $\epsilon_S = 80.0$ with ionic strength of 0.1 M and $\epsilon_p = 4.0$ for the protein interior.

To calculate the solvation energy ΔG_S^l (Eq. 4), electrostatic potentials are also needed for the homogeneous dielectric where $\epsilon_S = 4.0 = \epsilon_P$ for solvent and protein and vanishing ionic strength. In that case, the electrostatic potentials were evaluated simply by calculating the Coulomb energies for all atom pairs. For the inhomogeneous dielectric, the LPBE was solved in two focusing steps. The grid size was 242 Å and 140 Å for the "secondary" dimer and was 202 Å and 101 Å for the monomer, both with a grid spacing of 2.0 Å and 0.5 Å, respectively. To evaluate the mutual interactions, $W_{\mu\nu}$, of the titratable residues a finer grid is needed. Hence, the electrostatic potentials in the protein were calculated in three focusing steps. For the "secondary" dimer, the grid size was reduced from 242 Å via 107 Å to 18.75 Å with grid spacings of 2.0 Å, 1.0 Å, and 0.25 Å, respectively. For the monomer, grid sizes of 150 Å, 75 Å, and 18.75 Å were applied and the grid spacings were set to 2.0 Å, 1.0 Å, and 0.25 Å, respectively. For the model compounds, a grid size of 15 Å with a grid spacing of 0.25 Å was applied. The ionic strength was set to 0.1 M throughout. More details are given in Ullmann and Knapp (1999).

Monte Carlo sampling of conformations

In each MC sampling setup, a pair of protein configurations (two ASA monomers that are isolated and two ASA monomers that are associated to the "secondary" dimer) was investigated to establish the equilibrium distribution of the population between the configurations. The considered three pairs of configurations are the following: 1) two ASA monomers with Glu-424 in the conformation suitable for formation of the intramolecular hydrogen bond and the "secondary" dimer with Glu-424 in the same conformation; 2) two monomers where Glu-424 is in the conformation that corresponds to the intermolecular hydrogen bonds and the "secondary" dimer with the same conformation; and 3) two monomers with Glu-424 in the conformation that corresponds to the intramolecular hydrogen bond and the "secondary" dimer with the conformation of Glu-424 corresponding to the intermolecular hydrogen bonds. The latter pair accounts for the hypothesis that in the isolated monomer the conformation suitable for in-

tramolecular hydrogen bonds should be favorable and in the "secondary" dimer the conformation corresponding to intermolecular hydrogen bonds is predominating.

The MC titrations were performed with the program KARLSBERG (Rabenstein, 1999). Each pair of conformations was introduced into KARLSBERG simply as two conformations. Because the program requires that all conformations have the same number of titratable groups and to make sure that the reference energies refer to the proper reference conformations, we considered two noninteracting monomers in solution and one "secondary" dimer, respectively.

The MC titration was made at nine different pH values for each pair of configurations (monomer and "secondary" dimer) ranging from pH 3 to pH 11. Within one MC titration scan two attempts of configurational moves were made. Because the sampling of configurations was very inefficient, the poorly populated configuration was given a bias energy to raise the population, thereby increasing the sampling efficiency and reducing the statistical error. From the populations of both configurations the free energy difference between them can be calculated with Eq. 6. Because the bias energy is an additive constant, the bias can be simply removed by subtracting the bias energy from the free energy value calculated from Eq. 6.

However, the usage of a bias energy was not sufficient to yield a sampling efficiency that led to an acceptably small error level, which we considered to be fulfilled if the standard deviations in protonation probabilities were <0.01 for each titratable residue (Rabenstein et al., 1998). In addition, parallel tempering (Hansmann, 1997) had to be applied to raise the sampling efficiency. In the parallel tempering approach, the sampling is done simultaneously at different temperatures for which we used the following values: 300 K, 400 K, 530 K, 710 K, 950 K, 1266 K, and 1688 K. Within one MC titration scan, 20 tempering moves were made where the temperature of the considered configuration was changed. Initially, 1000 complete MC scans were made that included all titratable groups. Titratable groups that remained in a pure protonation state (fully protonated or unprotonated) and did not change their protonation state during the first 1000 MC scans were kept at their protonation state and were excluded from the list of titratable groups. With the resulting reduced set of titratable groups another 10,000 MC scans were made. This MC simulation procedure yielded a standard deviation of <0.01 protons at each titratable group.

Titration using the proton linkage model

To investigate the pH-dependent free energy of association by the proton linkage model, the monomer and the "secondary" dimer were titrated separately using the program KARLSBERG (Rabenstein, 1999). A major advantage of this method is that one can avoid the sampling problems, which arise by simulating the transitions between the monomer and dimer configurations. The same number of full and reduced MC scans were made as in the configurational sampling approach. The number of protons released upon association Δn(pH) is simply the difference of the total number of protons bound to the "secondary" dimer and to the individual monomers. Note that the number of protons bound to the monomer has to be doubled to be comparable to the number of protons bound to the dimer. The titration was made for the same six configurations (three isolated monomers and the corresponding three "secondary" dimer configurations) that were investigated in the configurational sampling approach. Because a numerical integration is required here (see Eq. 9), the titration for the proton linkage model was done in the pH interval from 3.0 to 11.0, with steps of 0.1 pH units.

RESULTS AND DISCUSSION

The protonation state of Glu-424

The suggested switch function of Glu-424 for the dimer-octamer association should result in a corresponding titration behavior of this residue in the four configurations (monomer versus dimer and intermolecular versus intramolecular hydrogen bonds involving Glu-424) that were investigated in this study. The titration curves for these four configurations are shown in Fig. 8. The titration properties of the two monomer structures are very similar. The protonation probability decreases from a value larger than 0.8 at pH 3.0 to a value of 0.0 at pH 7.0 (Fig. 8). The influence of the conformation of Glu-424 is very small for the titration behavior of the monomer (*solid* and *long-dashed lines* in Fig. 8). The conformation of Glu-424 that supports intramolecular hydrogen bonds behaves in the same way as the conformation, where Glu-424 points out into the solvent and is ready to form intermolecular hydrogen bonds in the "secondary" dimer configuration.

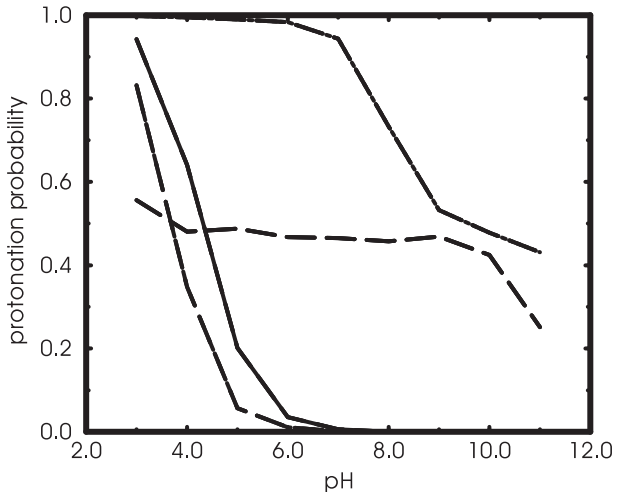

FIGURE 8 Protonation probability of Glu-424 in the monomer and the "secondary" dimer configuration. *Solid* and *long-dashed*: monomer configuration: *short-dashed* and *dashed-dotted lines*: "secondary" dimer configuration. GLU-INTRA conformation: *solid* and *short-dashed lines*; GLU-INTER conformation: *long-dashed* and *dashed-dotted lines*. For more details see text.

The titration curves of the dimers show a different behavior. Here, the conformation of Glu-424 suitable for the intermolecular hydrogen bonds shows a significantly higher protonation probability (*dash-dotted line* in Fig. 8) than the conformation that corresponds to the intramolecular hydrogen bond. Hence, the calculated titration curves support very well the formation of an intermolecular hydrogen bond with Phe-398–O in the "secondary" dimer, which requires a protonated Glu-424.

At high pH values, Glu-424 should preferentially be deprotonated. In the configuration of the "secondary" dimer, the acidic groups of the two Glu-424 are only 5 Å apart if they are in the conformation where they form intramolecular hydrogen bonds. However, to form the intramolecular hydrogen bonds both the Glu-424 need to be deprotonated. The Coulomb interaction due to the negative charges at the two glutamic acids renders this conformation

TABLE 1 Configurational energies for monomer-dimer association

Configurational Transition	$\Delta\Delta G_{conf}$
MONO/GLU-INTRA → DIMER/GLU-INTRA	−24.3
MONO/GLU-INTER → DIMER/GLU-INTER	−23.0
MONO/GLU-INTRA → DIMER/GLU-INTER	−23.2

Energies are computed for the reference protonation state according to Eq. 3. Energies are given in units of kcal/mol.

energetically very unfavorable. Hence, a deprotonation of the two Glu-424 is likely to go along with a dissociation of the "secondary" dimer that corresponds to the dissociation of the octamer into the "primary" dimers. However, as long as the monomers are forced to remain associated in the "secondary" dimer, as is done in the present computation, a complete deprotonation of Glu-424 does not occur. The importance of Glu-424 for the association process is also underlined by the observation that no other titratable group in the "secondary" dimer changes its protonation state significantly upon association. If one compares the protonation probabilities of all other titratable groups in the monomer state with those in the "secondary" dimer in the pH range from 3 to 11, the observed change is always <0.1. Only for Glu-424 the protonation probability varies considerably (depending on the pH and the conformation) by up to 0.9.

The association free energy by Monte Carlo sampling of configurations

To calculate the association energy on the basis of the population of the two different configurations evaluated by MC sampling (Eq. 6), their relative energies have to be considered in the reference protonation state where all titratable residues except histidine are in the neutral charge state. These energies do not depend on pH and the energy differences between each pair of configurations were found to be between −23.0 kcal/mol and −24.3 kcal/mol (Table 1). These energy values are nearly equal, although the individual contributions to these relative configurational energies are large numbers, as shown in Table 2. For the proportionality factor of the surface-dependent nonpolar contribution to the configurational energy, ΔG_{NE} in Eq. 5, we have chosen $\gamma = 20$ cal mol^{-1} Å^{-2}. Because the buried surface (II) of the interaction between the monomers in this study covers 900 Å^2, the change in solvent-accessible surface upon association is twice as large, leading to a contribution of 36 kcal/mol. This value is positive for the monomers, i.e., it favors association as the surface (II) decreases upon association. The chosen value of $\gamma = 20$ cal mol^{-1} Å^{-2} for the surface energy parameter is in agreement with data from the literature (Sitkoff et al., 1994; Zhang and Koshland, 1996). Because this empirical parameter value may not be applicable for all molecular systems in the same way, we suggest an alternative approach below.

TABLE 2 Individual contributions to conformational energies of monomer-dimer association

Conformation	ΔG_S	ΔG_{FF}	ΔG_{NE}	ΔG_{conf}
MONO/GLU-INTRA	−2866.04	−41926.53	36.00	−44263.87
MONO/GLU-INTER	−2378.06	−41922.01	36.00	−44264.07
DIMER/GLU-INTRA	−2866.04	−41422.12	0.00	−44288.17
DIMER/GLU-INTER	−2867.14	−41922.01	0.00	−44287.07

The energy terms are defined by Eq. 3 and the following equations. Energies are given in units of kcal/mol.

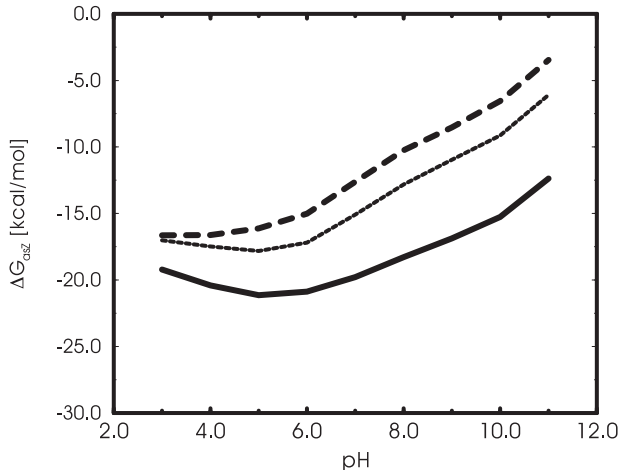

FIGURE 9 pH-Dependence of the free energy of association ΔG_{ass} of the monomers forming the "secondary" dimer. The energies obtained by MC simulation include conformational energy contributions according to Eq. 3 as displayed in Table 1. The solid (dashed) line refers to the conformation GLU-INTRA (DIMER/GLU-INTER), in which the Glu-424 is ready to form an intramolecular (intermolecular) hydrogen bond in the monomer and dimer state. The dotted line represents the data where the Glu-424 conformation is such that it forms the intramolecular hydrogen bond in the monomer state and the intermolecular hydrogen bond in the "secondary" dimer state, in agreement with the hypothesis on pH-dependent association.

The free energy of association of monomers to the "secondary" dimer is obtained by MC sampling and includes the configurational energy terms from Eq. 3, which were found to be pH-dependent (see Fig. 9). All association energies are negative, indicating that the association to the "secondary" dimer is energetically favorable at all pH values considered. In correspondence with the experimental finding, that at higher pH values the octamer dissociates to dimers, the association energy decreases with increasing pH value.

The association process with Glu-424 in the conformation suitable for intramolecular hydrogen bonding exhibits a minimum of the free energy around pH 6.0 (see Fig. 9, *solid line*). This is not consistent with the hypothesis that around pH 6 the "secondary" dimer should dissociate, which would require that the association energy is negative at lower pH values and positive at pH values higher than 6. This pH dependence indicates that association will not occur with

Glu-424 in the conformation where it forms the intramolecular hydrogen bonds. In addition, Fig. 8 shows that the protonation of both Glu-424, which is favorable for the association process, cannot be accomplished completely even at pH values below 5 if Glu-424 forms the intramolecular hydrogen bond. Hence, the present calculations suggest that Glu-424 has to adopt the conformation suitable for the intermolecular hydrogen bond to Phe-398–O to support the association process.

The pH dependence of the free energy of association shows a different behavior if Glu-424 is in a conformation that allows the formation of the intermolecular hydrogen bond to Phe-398–O. Here, the association energy shows no minimum, but increases monotonously with increasing pH value (Fig. 9, *dashed line*). In a more detailed treatment, the monomer state is considered with Glu-424 in the conformation suitable to form the intramolecular hydrogen bonds, whereas in the dimer state Glu-424 forms the intermolecular hydrogen bonds with Phe-398–O. The resulting pH dependence of the free energy of association appears roughly to be the arithmetic mean of the two other cases studied (Fig. 9, *dotted line*). In this case, there appears a shallow minimum at pH 5. Hence, the most probable conformation is where Glu-424 forms the intermolecular hydrogen bond in the "secondary" dimer configuration and remains in that conformation also in the monomer state, where it becomes solvent-exposed and forms appropriate hydrogen bonds with solvent molecules.

Because the computed free energies of association are always negative, the dissociation of the "secondary" dimer should not occur. This discrepancy with the experimentally found pH-dependent association behavior of ASA may be explained by the uncertainty of the nonelectrostatic contributions to the conformational energy (Eq. 3). Similar experiences were made before considering pH-dependent conformational changes in myoglobin (Rabenstein and Knapp, 2001) and the conformational gating process in bacterial photosynthetic reaction centers (Rabenstein et al., 2000). Table 2 shows that the contributions to the conformational energies yield large absolute values. They cancel to values of around −23 kcal/mol to −24 kcal/mol for the individual monomer-dimer pairs. Especially the surface energy parameter γ, which is responsible for the nonelectrostatic contribution to the solvation energy, may not be rigorously valid for all proteins as discussed above. To overcome the problem with the negative values of conformational energies we considered the observation that at around pH 6.0 the octamer dissociates into dimers. Therefore, we shifted all energies by a constant energy value such that at pH 6.0 the free energy of association vanishes. The resulting adjusted energy curves are visualized in Fig. 10.

The three curves of free energy of association for the GLU/INTRA, GLU/INTER, GLU/INTRA-INTER conformations had to be shifted by +20.8 kcal/mol, +15.0 kcal/mol, and +17.2 kcal/mol, respectively. As a consequence,

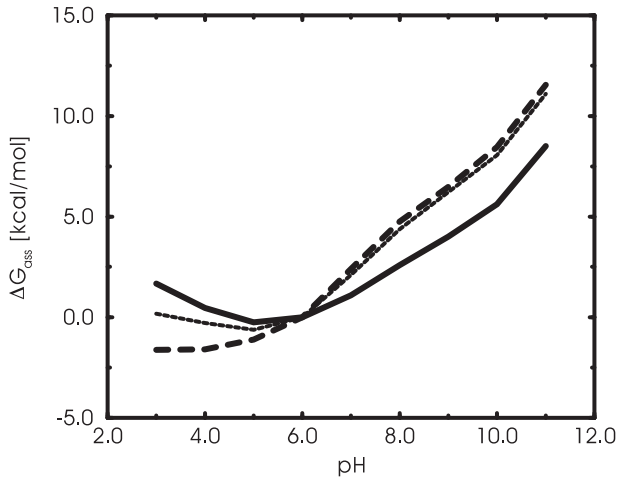

FIGURE 10 Free energy of association ΔG_{ass} to form the "secondary" dimer. The energies curves are shifted to obtain vanishing energies at pH 6 where, according to experiment, association occurs. The same notation as in Fig. 9 is used. More details are given in text.

the conformational energies should be less negative. The corresponding corrected conformational energies are listed in Table 3. The correction of the conformational energies can be rationalized by uncertainties of the surface energy term. The initially chosen value of $\gamma = 20.0$ cal mol^{-1} Å^{-2} was obtained by considering completely hydrophobic surfaces consisting exclusively of ethyl- and propyl-like groups (Zhang and Koshland, 1996). However, the dimer-dimer interface (II) of ASA is formed by 21 residues, of which 12 are hydrophobic, suggesting that a reduction of the surface energy parameter to 50–60% of its initial value would be necessary. To obtain a vanishing free energy of association at pH 6.0, we adjusted the conformational energy difference between the isolated monomers and "secondary" dimer configuration, yielding surface energy parameters γ in the range from 8.4 cal mol^{-1} Å^{-2} to 11.6 cal mol^{-1} Å^{-2} (Table 3), which correspond well to a reduction of ~50%. With these adopted surface energy parameters the nonpolar (pH-independent) contribution of the association energy at the "secondary" dimer interface (II) of ASA amounts to ~−18 kcal/mol. Because at pH 5 the association energy is only ~−2 kcal/mol (see Fig. 9), it can be deduced that the

TABLE 3 Adjusted difference of conformational energies and surface energy parameters γ

Conformational Transition	$\Delta\Delta G_{conf}$	γ
MONO/GLU-INTRA → DIMER/GLU-INTRA	−3.5	8.4
MONO/GLU-INTER → DIMER/GLU-INTER	−8.0	11.6
MONO/GLU-INTRA → DIMER/GLU-INTER	−6.2	9.3

Energies were obtained by adjusting the zero point of the energies of association at pH 6, where monomer and dimer state should have the same free energy. Energies are given in units of kcal/mol.

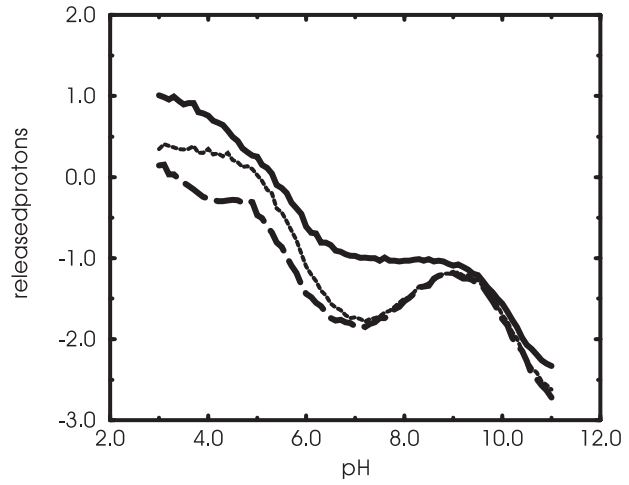

FIGURE 11 Proton release upon association of ASA monomers to the "secondary" dimer at different pH values. *Solid line:* GLU/INTRA; *dashed line:* GLU/INTER; *dotted line:* GLU/INTRA-INTER. For more details see text.

electrostatic contribution to the association energy opposes binding.

Results on ASA association from the proton linkage model

The key parameter that is used in the proton linkage model is the release/uptake of protons upon association of monomers to dimers. This is the difference between the number of protons bound to two isolated monomers and the number of protons bound to the corresponding dimer. The difference of the number of protons as a function on pH can be seen in Fig. 11 for the three ASA monomer-dimer pairs described in the Methods section. Integrating the pH-dependent number of protons starting from the pH value pH_1 with a known equilibrium constant until an arbitrary second pH value pH_2 leads to the equilibrium constant at pH_2 according to Eq. 9. In the present application, the association constant at pH 6.0 is chosen to be 1.0, because it is known experimentally that ASA associates to the octamer corresponding to the "secondary" dimer at pH values between 5 and 7. The free energies of association are determined from the equilibrium constants via Eq. 10. The results from the direct MC sampling method simulating the configurational transitions between isolated monomer and "secondary" dimer states have converged. Hence, it is not surprising that the pH-dependent free energy curves computed with the proton linkage model perfectly agree with results obtained by the direct method used to compute the free energy of association. The free energies of association obtained from the proton linkage model are therefore not shown explicitly.

CONCLUSIONS

The present calculations show that the pH-dependent association of ASA dimers to octamers occurs at low pH with the protonated Glu-424 in a conformation suitable to form intermolecular hydrogen bonds with Phe-398–O, as was also suggested by the crystal structure analysis. The computational results for the ASA dimer at high pH (above pH 6) are less conclusive. There is only a small energy difference between the conformation of the unprotonated Glu-424 forming an intramolecular hydrogen bond with Gln-460 where Glu-424 is partially buried and the solvent exposed conformation where Glu-424 would be ready to form the intermolecular hydrogen bond in the octamer state with a small preference for the latter conformation. The switch function of Glu-424 would then be restricted to the change in the protonation state, when the pH value is changed.

Technically, it was possible to simulate the dimer-octamer association by considering just two monomers merging at the interface (II) to form the "secondary" dimer. In this way, the size of the molecular system for which the Poisson-Boltzmann equation needed to be solved could be considerable reduced. We encountered severe sampling problems during the MC simulation of the association process. These could be overcome only by introducing an energetic bias to populate the monomer and "secondary" dimer configurations more evenly and by the usage of the parallel tempering method where configurational transitions are facilitated by simultaneously sampling monomer-dimer ensembles at a number of elevated temperatures. Alternatively, we applied the proton linkage model, where one can avoid the MC simulation of the transition between monomer and "secondary" dimer state completely, and obtained results matching with the direct MC simulation method.

Using a conventional surface energy term that is proportional to the loss of solvent-exposed surface area with a proportionality factor $\gamma = 20$ cal mol^{-1} Å^{-2}, the absolute values of free energy of association are negative throughout, which means that the octamer should be more stable than the dimer for all pH values. However, the surface energy parameter was determined for purely hydrophobic compounds. We adjusted the surface energy contribution by an additive constant to obtain a vanishing association energy at pH 6. It yields $\gamma = 11.6$ cal mol^{-1} Å^{-2} if Glu-424 is in a conformation suitable to form intermolecular hydrogen bonds in dimer and octamer states, and it yields $\gamma = 9.3$ cal mol^{-1} Å^{-2} if Glu-424 is forming intramolecular hydrogen bonds in the dimer state and intermolecular hydrogen bonds in the octamer state. These reduced values of the surface energy parameter γ are in agreement with the fraction of hydrophobic residues lying in the interface (II) of the dimer-octamer association, which is $<60\%$.

Investigation of the different energy contributions to ASA association shows that the surface energy is the driving force of the association process. The electrostatic energy

opposes association, presumably because the protonation of Glu-424 that is needed to form the intermolecular hydrogen bond is energetically unfavorable at pH 6, where the dimer-octamer association occurs. However, due to the pH dependence of the electrostatic repulsion, the electrostatic interaction is the steering force of the association process.

We thank Dr. Donald Bashford and Dr. Martin Karplus for providing the programs MEAD and CHARMM22, respectively. We thank Björn Rabenstein for useful discussions.

This work was supported by the Deutsche Forschungsgemeinschaft SFB 498, Projects A4 and A5, the Graduate Colleges GRK 80/2, GRK 268, and GRK 788/1, and by the Fonds der Chemischen Industrie and BMFT.

REFERENCES

Ballabio, A., and L. J. Shapiro. 1995. Steroid sulfatase deficiency and *X*-linked ichthyosis. *In* The Metabolic and Molecular Bases of Inherited Disease. C. R. Shriver, A. L. Beaudet, W. S. Sly, and D. Valle, editors. McGraw-Hill, New York. 2999–3022.

Bashford, D. 1997. An object oriented programming suite for electrostatic effects in biological molecules. *In* Scientific Computing in Object-Oriented Parallel Environments. Y. Ishikawa, R. R. Oldehoeft, J. V. W. Reynders, and M. Tholburn, editors. Springer, Berlin. 233–240.

Bashford, D., and K. Gerwert. 1992. Electrostatic calculations of the pK_a values of ionizable groups in bacteriorhodopsin. *J. Mol. Biol.* 224: 473–486.

Beroza, P., M. Y. Fredkin, M. Y. Okamura, and G. Feher. 1995. Electrostatic calculation of amino acid titration and electron transfer QAQB-QAQB in the reaction center. *Biophys. J.* 68:2233–2250.

Bogan, A. A., and K. S. Thorn. 1998. Anatomy of hot spots in protein interfaces. *J. Mol. Biol.* 280:1–9.

Brooks, B. R., R. E. Bruccoleri, B. D. Olafson, D. J. States, S. Swaminathan, and M. Karplus. 1983. CHARMM: a program for macromolecular energy, minimization and dynamics calculations. *J. Comp. Chem.* 4:187–217.

Chothia, C. 1976. The nature of accessible and buried surfaces in proteins. *J. Mol. Biol.* 105:1–14.

Coleman, J. E. 1992. Structure and mechanism of alkaline phosphatase. *Annu. Rev. Biophys.* 21:441–483.

Collaborative Computational Project Number 4. 1994. The CCP4 Suite: Programs for Protein Crystallography. *Acta Crystallogr. D.* 50:760–763.

Dierks, T., B. Schmidt, and K. von Figura. 1997. Conversion of cysteine to formylglycine: a protein modification in the endoplasmatic reticulum. *Proc. Natl. Acad. Sci. U.S.A.* 94:11963–11968.

Eisenberg, D., and A. McLachlan. 1986. Solvation energy in protein folding and binding. *Nature.* 319:199–203.

Elcock, A. H., R. R. Gabdoulline, R. C. Wade, and J. A. McCammon. 1999. Computer simulation of protein-protein association kinetics: acetylcholinesterase-fasciculin. *J. Mol. Biol.* 291:149–162.

Franco, B., G. Meroni, G. Parenti, J. Levilliers, L. Bernard, M. Gebbia, L. Cox, P. Maroteaux, L. Sheffield, G. A. Rappold, G. Andria, C. Petit, and A. Ballabio. 1995. A cluster of sulfatase genes on Xp22.3: mutations in chondrodysplasia punctata (cdpx) and implications for warfarin embryopathy. *Cell.* 81:15–25.

Gavin, A. C., M. Bosche, R. Krause, P. Grandi, M. Marzioch, A. Bauer, J. Schultz, J. M. Rick, A. M. Michon, C. M. Cruciat, M. Remor, C. Hofert, M. Schelder, M. Brajenovic, H. Ruffner, A. Merino, K. Klein, M. Hudak, D. Dickson, T. Rudi, V. Gnau, A. Bauch, S. Bastuck, B. Huhse, C. Leutwein, M. A. Heurtier, R. R. Copley, A. Edelmann, E. Querfurth, V. Rybin, G. Drewes, M. Raida, T. Bouwmeester, P. Bork, B. Seraphin, B. Kuster, G. Neubauer, and G. Superti-Furga. 2002. Functional organization of the yeast proteome by systematic analysis of protein complexes. *Nature.* 415:141–147.

Getzoff, E. D., D. E. Cabelli, C. L. Fisher, H. E. Parge, M. E. Viezzoli, L. Banci, and R. A. Hallewell. 1992. Faster superoxide dismutase reaction mutants designed by enhancing electrostatic guidance. *Nature.* 358: 347–351.

Gilson, M. K., A. Rashin, R. Fine, and B. Honig. 1985. On the calculation of electrostatic interactions in proteins. *J. Mol. Biol.* 183:503–516.

Hansmann, U. H. E. 1997. Parallel tempering algorithm for conformational studies of biological molecules. *Chem. Phys. Lett.* 281:140–150.

Hendsch, Z. S., and B. Tidor. 1994. Do salt bridges stabilize proteins? A continuum electrostatic analysis. *Protein Sci.* 3:211–226.

Honig, B., and W. L. Hubbell. 1984. Stability of salt bridges in membrane proteins. *Proc. Natl. Acad. Sci. U.S.A.* 81:5412–5416.

Honig, B., and A. Nicholls. 1995. Classical electrostatics in biology and chemistry. *Science.* 268:1144–1149.

Honig, B., and A-S. Yang. 1995. Free energy balance in protein folding. *Adv. Protein Chem.* 46:27–58.

Jerfy, A., A. B. Roy, and H. J. Tomkins. 1976. The sulfatase of ox liver. XIX. On the nature of polymeric forms of sulfatase A present in dilute solutions. *Biochim. Biophys. Acta.* 422:335–348.

Jones, S., and J. M. Thornton. 1996. Principles of protein-protein interactions. *Proc. Natl. Acad. Sci. U.S.A.* 93:13–20.

Kolodny, E. H., and A. R. Fluharty. 1995. Methachromatic leukodystrophy and multiple sulfatase deficiency sulfatide lipidosis. *In* The Metabolic and Molecular Bases of Inherited Disease. C. Shriver, A. L. Beaudet, W. S. Sly, and D. Valle, editors. McGraw-Hill, New York. 2693–2741.

Kraulis, P. J. 1991. MOLSCRIPT: a program to produce both detailed and schematic plots of protein structures. *J. Appl. Crystallogr.* 24:946–950.

Larsen, T. A., A. J. Olson, and D. S. Goodsell. 1998. Morphology of protein-protein interfaces. *Structure.* 6:421–427.

Laskowsky, M., and R. Finkenstadt. 1972. Study of protein-protein and of protein-ligand interaction by potentiometric methods. *Methods Enzymol.* 26:193–227.

Lebovitz, J., and M. Laskowsky. 1962. Potentiometric measurement of protein-protein association constants. Soybean trypsin inhibitor-trypsin association. *Biochemistry.* 1:1044–1055.

Lo Conte, L., C. Chothius, and J. Janin. 1999. The atomic structure of protein-protein recognition sites. *J. Mol. Biol.* 285:2177–2198.

Lukatela, G., N. Krauss, K. Theis, T. Selmer, V. Gieselmann, K. von Figura, and W. Saenger. 1998. Crystal structure of human arylsulfatase A: the aldehyde function and the metal ion at the active site suggest a novel mechanism for sulfate ester hydrolysis. *Biochemistry.* 37: 3654–3664.

MacKerrell, J. A. D., D. Bashford, M. Bellot, J. R. L. Dunbrack, J. D. Evanseck, M. J. Field, S. Fischer, J. Gao, H. Guo, S. Ha, D. Joseph-McCarthy, L. Kuchnir, K. Kuczera, F. T. K. Lau, C. Mattos, S. Michnick, T. Ngo, D. T. Nguyen, B. Prodholm, W. E. Reiher III, B. Roux, M. Schlenkrich, J. C. Smith, R. Stote, J. Straub, M. Watanabe, J. Wiórkiewicz-Kuczera, D. Yin, and M. Karplus. 1998. All-atom empirical potential for molecular modeling and dynamics studies of proteins. *J. Phys. Chem. B.* 102:3586–3616.

Mauk, M. R., P. D. Barker, and A. G. Mauk. 1991. Proton linkage of complex formation between cytochrome c and cytochrome b_5: electrostatic consequences of protein-protein interactions. *Biochemistry.* 30: 9873–9881.

Mauk, M. R., J. C. Ferrer, and A. G. Mauk. 1994. Proton linkage in formation of the cytochrome-c-cytochrome-c-peroxidase complex: electrostatic properties of the high and low affinity cytochrome binding sites on the peroxidase. *Biochemistry.* 33:12609–12614.

McPherson, P. H., M. Y. Okamura, and G. Feher. 1988. Light-induced proton-uptake by photosynthetic reaction centers from *Rhodobacter spheroides* r-26. I. Protonation of one electron states DQA, DQA, DQAQB and DQAQB. *Biochim. Biophys. Acta.* 934:309–324.

Neufeld, E. F., and J. Muenzer. 1995. The mucopoly saccharidoses. *In* The Metabolic and Molecular Bases of Inherited Disease. C. R. Shriver, A. L. Beaudet, W. S. Sly, and D. Valle, editors. McGraw-Hill, New York. 2465–2494.

Nichol, L. W., and A. B. Roy. 1965. The sulfatase of ox liver. 9. The polymerization of sulfatase A. *Biochemistry.* 4:386–396.

Nichol, L. W., and A. B. Roy. 1966. The sulfatase of ox liver. X. Some observations on the intermolecular binding in sulfatase A. *Biochemistry.* 5:1379–1388.

Nicholls, A., and A. B. Roy. 1971. The Enzymes. Academic Press, New York. 21–41.

Nozaki, Y., and C. Tanford. 1971. The solubility of amino acids and two glycine peptides in aqueous ethanol and dioxane solutions. Establishment of a hydrophobicity scale. *J. Biol. Chem.* 246:2211–2217.

Parseghian, V. 1969. Energy of an ion crossing a low dielectric membrane: solutions to four relevant electrostatic problems. *Nature.* 221:844–846.

Rabenstein, B. 1999. KARLSBERG online manual. Freie Universität, Berlin.

Rabenstein, B., and E. W. Knapp. 2001. Calculated pH-dependent population and protonation of CO-myoglobin conformers. *Biophys. J.* 80: 1141–1150.

Rabenstein, B., G. M. Ullmann, and E. W. Knapp. 1998. Energetics of electron transfer and protonation reactions of the quinones in the photosynthetic reaction center of *Rhodopseudomonas viridis*. *Biochemistry.* 37:2488–2495.

Rabenstein, B., G. M. Ullmann, and E. W. Knapp. 2000. Electron transfer between the quinones in the photosynthetic reaction center and its coupling to conformational changes. *Biochemistry.* 39:10487–10496.

Reddy, V. S., H. A. Giesing, R. Morton, A. Kumar, C. B. Post, C. L. I. Brooks, and J. E. Johnson. 1998. Energetics of quasi-equivalence: computational analysis of protein-protein interactions in icosahedral viruses. *Biophys. J.* 74:546–558.

Schaefer, M., and M. Karplus. 1997. pH-Dependence of protein stability: absolute electrostatic free energy differences between conformations. *J. Phys. Chem. B.* 101:1663–1683.

Schapira, M., M. Totrov, and R. Abagyan. 1999. Prediction of the binding energy for small molecules, peptides and proteins. *J. Mol. Recognit.* 12:177–190.

Sharp, K., R. Fine, and B. Honig. 1987. Computer simulations of the diffusion of a substrate to an active site of an enzyme. *Science.* 236: 1460–1463.

Sheinerman, F. B., R. Norel, and B. Honig. 2000. Electrostatic aspects of protein-protein interactions. *Curr. Opin. Struct. Biol.* 10:153–159.

Sitkoff, D., K. A. Sharp, and B. Honig. 1994. Accurate calculation of hydration free energies using macroscopic solvent models. *J. Phys. Chem.* 98:1978–1988.

Tanford, C. 1970. Protein denaturation. Part C. Theoretical models for the mechanism of denaturation. *Adv. Protein Chem.* 25:1–95.

Ullmann, G. M., and E. W. Knapp. 1999. Electrostatic models for computing protonation and redox equilibria in proteins. *Eur. Biophys. J.* 28:533–551.

Vallee, B. L., and D. S. Auld. 1993. New perspective on zinc biochemistry: catalytic sites in multi-zinc enzymes. *Biochemistry.* 32:6493–6500.

van Vlijmen, H. W. T., S. Curry, M. Schaefer, and M. Karplus. 1998. Titration calculations of foot-and-mouth disease virus capsids and their stability as a function of pH. *J. Mol. Biol.* 275:295–308.

Waheed, A., and R. L. van Etten. 1979. The monomer-dimer association of rabbit liver aryl sulfatase A and its relationship to anomalous kinetics. *Arch. Biochem. Biophys.* 194:215–225.

Waheed, A., and R. L. van Etten. 1985. Purification of mammalian arylsulfatase A enzymes by subunit affinity chromatography. *Int. J. Pept. Protein Res.* 26:362–372.

Wyman, J. 1964. Linked functions and reciprocal effects in hemoglobin: a second look. *Adv. Protein Chem.* 19:223–286.

Xiao, L., and B. Honig. 1999. Electrostatic contribution to the stability of hyperthermophilic proteins. *J. Mol. Biol.* 289:1435–1444.

Xu, D., S. L. Lin, and R. Nussinov. 1997. Protein binding versus protein folding: the role of hydrophilic bridges in protein association. *J. Mol. Biol.* 265:68–84.

Yang, A-S. 1993. On the pH dependence of protein stability. *J. Mol. Biol.* 231:459–474.

Yang, A-S., and B. Honig. 1995. Free energy determinants of secondary structure formation. II. Antiparallel b-sheets. *J. Mol. Biol.* 252:366–376.

Zhang, T., and J. D. E. Koshland. 1996. Computational method for relative binding energies of enzyme substrate complexes. *Protein Sci.* 5:348–356.